The EMBO Journal Vol.18 No.13 pp.3757–3766, 1999

Polyadenylation accelerates the degradation of the mitochondrial mRNA associated with cytoplasmic male sterility in sunflower

Dominique Gagliardi and Christopher J.Leaver[1]

Department of Plant Sciences, University of Oxford, South Parks Road, Oxford OX1 3RB, UK

[1]Corresponding author
e-mail: chris.leaver@plants.ox.ac.uk

In sunflower, PET1-cytoplasmic male sterility is correlated with the presence of a novel mitochondrial gene (*orf522*) located 3′ to the *atpA* gene. The dicistronic atpA-orf522 transcripts are preferentially destabilized in male florets of 'restored to fertility' plants as compared with sterile plants. In this report, we show that atpA-orf522 transcripts may be polyadenylated *in vivo* at their 3′ termini and that a tissue-specific increase in the level of polyadenylated atpA-orf522 transcripts correlates with the tissue-specific instability of atpA-orf522 mRNAs in male florets of the restored hybrid plants. In addition, we have identified two distinct ribonuclease activities in sunflower mitochondria, one of which preferentially degrades polyadenylated as compared with non-polyadenylated RNA substrates corresponding to the 3′ UTR of atpA-orf522 transcripts. These *in vivo* and *in vitro* results show that polyadenylation is involved in the degradation pathway of the mitochondrial atpA-orf522 transcripts and that polyadenylation can be developmentally regulated by a nuclear gene(s) upon restoration of fertility.

Keywords: cytoplasmic male sterility/plant mitochondria/polyadenylation/RNA degradation/sunflower

Introduction

Polyadenylation at the 3′ end of mRNAs is a widespread post-transcriptional modification that has been extensively studied for nuclear-encoded transcripts (Manley and Proudfoot, 1994). It is now assumed that in eukaryotes, poly(A) tails play essential roles in the stability and the translation initiation of the overall majority of nuclear-encoded mRNAs (Manley and Proudfoot, 1994). The addition of poly(A) sequences to RNAs has also been well characterized in mitochondria of mammals and trypanosomes. Most of the processed mammalian mitochondrial mRNAs terminate with U or UA and a functional translation stop codon is created by polyadenylation (Ojala *et al*., 1981). In *Trypanosoma brucei*, the majority of mitochondrial mRNAs are present as two size classes due to varying lengths of their 3′ poly(A) tails (Bhat *et al*., 1992). The exact role of polyadenylation of mitochondrial mRNAs in trypanosomes is unclear and it can occur independently of other RNA editing and processing events (Koslowsky and Yahampath, 1997). Yeast mitochondrial RNAs may also contain a short polyadenylic acid segment (Hendler *et al*., 1975), although to our knowledge these findings have not been confirmed and the role of polyadenylation in yeast mitochondria has not been determined. In contrast, polyadenylation of RNAs in bacteria (for a review see Sarkar, 1997) and in chloroplasts (Kudla *et al*., 1996; Lisitsky *et al*., 1996) is a much better understood process. Addition of poly(A) tracts to 3′ termini and to the 3′ termini generated by endonucleolytic cleavage of RNAs results in their rapid degradation in bacteria (Ohara *et al*., 1995; Xu and Cohen, 1995; Haugel-Nielsen *et al*., 1996; Ingle and Kushner, 1996; Söderbom and Wagner, 1998; Szalewska-Palasz *et al*., 1998) as well as in chloroplasts (Kudla *et al*., 1996; Lisitsky *et al*., 1996, 1997a). In both systems, reduction or inhibition of polyadenylation reduces the rate of the RNA degradation (Ingle and Kushner, 1996; Lisitsky *et al*., 1997b).

RNA degradation is thought to play an important role in the control of mitochondrial genome expression in higher plants (Finnegan and Brown, 1990; Mulligan *et al*., 1991) but is still a poorly understood process. Some mitochondrial transcripts contain inverted repeat sequences in their 3′ region that can be predicted to fold into stem–loop structures (Schuster *et al*., 1986). It has recently been shown that these stem–loops do not act as transcription terminators but rather as processing signals (Dombrowski *et al*., 1997). In addition, Bellaoui *et al*. (1997) have shown that secondary structures located at the 3′ termini of mitochondrial transcripts are important determinants of stability for a specific mRNA. As an experimental protocol for transforming higher plant mitochondria has yet to be developed, naturally occurring or induced mutations in mitochondrial DNA are invaluable tools for the study of the control of plant mitochondrial genome expression. The best-characterized mitochondrial mutations are those which result in cytoplasmic male sterility (CMS). CMS is a maternally inherited trait recognized by the failure of the plant to produce functional pollen. CMS has been described in >150 plant species, and in the best-characterized systems CMS is associated with aberrant recombination events in the mitochondrial genome which result in the generation of novel open reading frames that are expressed as variant polypeptides (Schnable and Wise, 1998). Male fertility can be restored by the introduction in a cross of nuclear genes, usually termed *Rf* genes for restorer of fertility (Schnable and Wise, 1998). Nuclear restoration of fertility thus provides a good experimental system in which to study nuclear–mitochondrial interactions. In sunflower (*Helianthus annuus*), PET1-CMS was obtained from an interspecific cross between *Helianthus petiolaris* and *H.annuus* and is associated with the presence of a novel mitochondrial gene, *orf522*, which encodes a 16 kDa polypeptide (Monéger *et al*., 1994). The *orf522* gene was created by a recombination event

involving an inversion/insertion rearrangement 3′ to the *atpA* gene (Köhler *et al*., 1991; Laver *et al*., 1991). The sterile line is characterized by the presence of atpA-orf522 dicistronic mRNAs in addition to the monocistronic atpA transcripts present in the fertile line (Köhler *et al*., 1991; Laver *et al*., 1991). Interestingly, the steady-state level of atpA-orf522 transcripts is reduced upon restoration of fertility in a tissue-specific manner as this reduction is only observed in male florets of restored hybrid plants and not in vegetative tissues of these plants (Monéger *et al*., 1994; Smart *et al*., 1994). As the transcription rate of the *orf522* gene is identical in sterile and restored hybrid male florets, it was concluded that atpA-orf522 transcripts are preferentially destabilized in a tissue-specific manner upon restoration of fertility (Monéger *et al*., 1994).

In this paper, we show that atpA-orf522 transcripts may be polyadenylated *in vivo* at their 3′ termini and that polyadenylation occurs in cotyledons as well as in male florets. However, an increase in the relative level of polyadenylated atpA-orf522 transcripts is correlated with the tissue-specific instability of atpA-orf522 mRNAs in male florets of restored hybrid plants. In addition, we have characterized and separated by fast-performance liquid chromatography (FPLC) two distinct ribonuclease activities from sunflower mitochondria. One of these ribonuclease activities degrades polyadenylated RNAs at a faster rate as compared with non-polyadenylated RNAs, while the other ribonuclease activity is independent of the polyadenylation status of the RNA substrate. The respective roles of these two distinct ribonuclease activities is discussed. We conclude from our *in vivo* and *in vitro* results that polyadenylation is involved in the degradation pathway of the mitochondrial mRNA associated with cytoplasmic male sterility in sunflower and that the polyadenylation status of these transcripts is modulated during development by a nuclear gene(s) upon restoration of fertility.

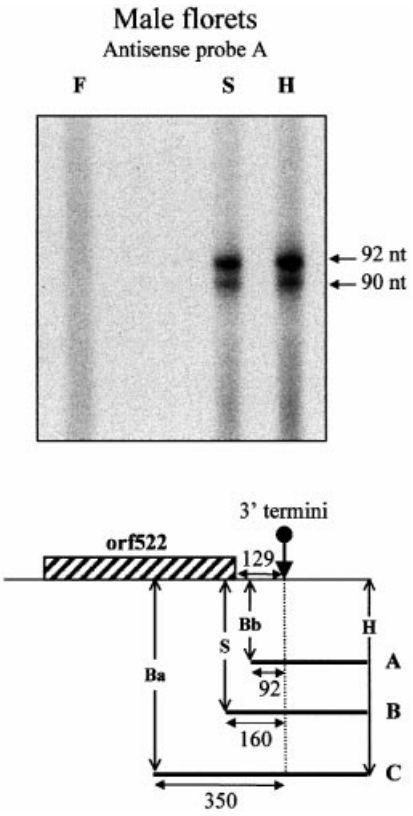

Fig. 1. The 3′ ends of mature atpA-orf522 transcripts are identical in male florets of sterile and restored hybrid plants. RNase protection experiments were carried out using fertile (F), sterile (S) or restored hybrid (H) male floret total RNA and three radiolabelled *in vitro* transcribed antisense RNA probes: A, B and C (see Materials and methods). The location of the probes and the restriction enzyme sites are indicated on the scheme. Ba, *Bam*HI; S, *Sca*I; Bb, *Bbv*I; H, *Hinc*II. Sizes are indicated in nucleotides. The upper part of the figure presents the results obtained using the antisense probe A. Note that the amount of the radiolabelled probe was limiting in this experiment.

Results

The 3′ termini of mature atpA-orf522 transcripts are identical in male florets from sterile and restored hybrid plants

It has recently been shown that the stability of mRNAs from the Ogura CMS locus in *Brassica* cybrids is determined by the secondary structure of the 3′ UTR of the transcripts (Bellaoui *et al*., 1997). These observations suggest that the preferential degradation of atpA-orf522 transcripts in male florets of the restored hybrid sunflower plants could be due to differences in the sequence/structure of the 3′ UTRs of these transcripts. Such alternative 3′ UTRs may be the consequence of a different processing of the 3′ UTR or tissue-specific organization of the mitochondrial DNA. Stoichiometric shifts in independently replicating subgenomic DNA molecules containing the CMS locus have been observed upon restoration to fertility or spontaneous reversion to fertility in *Phaseolus vulgaris* CMS (Janska *et al*., 1998). However, we have shown by Southern blot analysis that the mitochondrial DNA organization at the *orf522* locus is identical in sterile and restored hybrid male florets (results not shown). To test the possibility of differential processing in the 3′ UTR of atpA-orf522 transcripts, we have mapped the 3′ termini of the atpA-orf522 transcripts in male florets of sterile and restored hybrid plants by RNase protection. We used three different antisense RNA probes, the position and length of which are indicated in the scheme in Figure 1. In all these experiments, no RNA was protected in male florets of fertile plants which do not contain the *orf522* gene (see Figure 1 for the results obtained using the shortest of the three antisense RNA probes, denoted A). The antisense RNA probe A was chosen to allow the protection of a short fragment of <100 ribonucleotides of the 3′ UTR (Figure 1). The major 3′ end of atpA-orf522 transcripts was estimated to be located 129 nucleotides 3′ of the orf522 stop codon. A minor 3′ end is detected 127 nucleotides 3′ to the orf522 stop codon. The sizes and relative proportion of the two protected fragments (~90 and ~92 nucleotides) are identical in sterile and restored hybrid plants (Figure 1). We confirmed using antisense RNA probes B and C that the 3′ termini of atpA-orf522 transcripts are identical in male florets from sterile and restored hybrid plants (results not shown). We conclude from these experiments that the instability of atpA-orf522 mRNAs in male florets of restored hybrid plants is not due to differential 3′ processing of these transcripts.

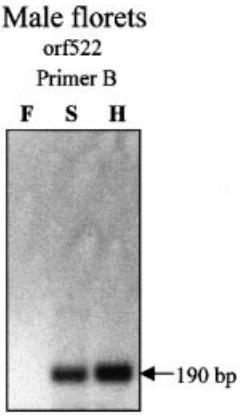

Fig. 2. Detection of polyadenylated atpA-orf522 transcripts by RT–PCR. Negative image of an ethidium bromide-stained gel of PCR products amplified using the orf522-specific primer B in combination with the adapter primer. cDNAs were synthesized using an oligo(dT)$_{18}$-adapter primer from mitochondrial RNAs isolated from male florets of fertile (F), sterile (S) and restored hybrid (H) plants.

Table I. List of PCR primers

Oligo(dT)$_{18}$-adapter primer	CGACCCTCGAGAGGATCCCG(T)$_{18}$
Adapter primer	CGACCCTCGAGAGGATCCCG
orf522-specific primer A	GGGATCCGTCCTTGCGTGAGGGTTTG
orf522-specific primer B	GGGTACCGAGAACGGTACTCATAG
orf522-specific primer C	GGGTACCTTATTCGTATTATGAGG
orf522-specific primer D	GGCTCGAGTCAGATTATGAACCCCAA
atp6-specific primer	AGGTACCGAATGATGCTATAAATC

The underlined nucleotides in the gene-specific primers do not correspond to gene sequences but have been added for cloning purposes.

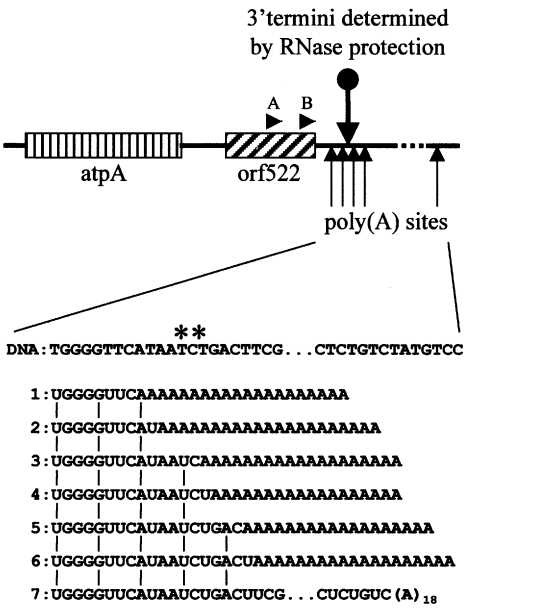

Fig. 3. atpA-orf522 transcripts may be polyadenylated *in vivo* at their 3′ termini. The scheme in the upper part of the figure depicts the organization of *atpA* and *orf522* genes in the mitochondrial DNA of sterile and restored hybrid plants (not to scale). The location and orientation of primers A and B are shown by arrowheads. The polyadenylation sites are marked by the lower thin arrows. The position of the mature 3′ termini of atpA-orf522 mRNAs determined in Figure 1 are indicated by the upper thick arrow in the scheme and by asterisks in the DNA nucleotide sequence shown below. Details of the seven different sequences obtained from 20 polyadenylated cDNA clones are shown.

The 3′ termini of atpA-orf522 transcripts may be polyadenylated in vivo

To date no evidence has been published that mature mitochondrial RNAs are polyadenylated in plants. This was previously also thought to be the case for the bulk of bacterial and chloroplast RNAs. However, it has been shown recently that RNAs are targeted for degradation by polyadenylation in both of these systems (Kudla *et al*., 1996; Lisitsky *et al*., 1996; for a review of bacterial RNA polyadenylation see Sarkar, 1997). To investigate whether polyadenylation of mRNAs does occur in plant mitochondria, total mitochondrial RNA was isolated from male florets of fertile, sterile and restored hybrid sunflower plants and reverse-transcribed using an oligo(dT)$_{18}$-adapter primer. The resulting first strand cDNAs were subjected to PCR amplification using a primer corresponding to the adapter primer and a primer specific for the orf522 sequence (primer B in Figure 3) (see Table I for all primer sequences). Discrete PCR products of 190 bp were amplified from cDNAs prepared from both sterile and restored hybrid plants (Figure 2, lanes S and H). No signal was detected using cDNA prepared from mitochondrial RNAs from fertile male florets with the orf522 specific primer B (Figure 2, lane F). The PCR amplification products were cloned and sequenced. An analysis of 20 clones shows that 19 clones correspond to the 3′ termini of atpA-orf522 transcripts followed by a stretch of adenosine residues (Figure 3). A single clone contained a poly(A) sequence located 324 nucleotides 3′ to the stop codon. All the clones analysed contain a poly(A) sequence of 17–21 nucleotides which corresponds approximately to the length of the oligo(dT) primer used for cDNA synthesis. We are nevertheless certain that these sequences represent genuine *in vivo* polyadenylated transcripts for the following reasons. First, the PCR products cannot have been amplified from contaminating mitochondrial DNA, as RNAs were treated extensively with DNase I before cDNA synthesis and because the sequence of the PCR adapter primer does not contain any deoxythymidine residues at its 3′ end (see Table I). Thus, the observed poly(A) sequences must originate from cDNA synthesis. Secondly, as a control to check the possibility that the oligo(dT)$_{18}$-adapter primer could artefactually prime RNAs corresponding to non-polyadenylated 3′ termini of atpA-orf522 transcripts, the following experiment was performed. RNAs corresponding to non-polyadenylated or polyadenylated 3′ UTRs of atpA-orf522 transcripts were transcribed *in vitro* from the clone 3 in Figure 3 using a strategy similar to the one described in Materials and methods for the clone 5 in Figure 3. After extensive digestion by DNase I, the *in vitro* transcribed RNAs were reverse-transcribed using the oligo(dT)$_{18}$-adapter primer and subjected to PCR amplification using the adapter primer and orf522-specific primer B. As shown in Figure 4, no PCR product was amplified from cDNA corresponding to non-polyadenylated 3′ UTR of atpA-orf522 transcripts. The third factor that convinced us of the existence of genuine *in vivo* polyadenylated atpA-orf522 transcripts is the location of the polyadenylation sites. The poly(A) tails of 19 out of 20 clones are not widely distributed in the 3′ UTR of atpA-orf522 transcripts but are located at six

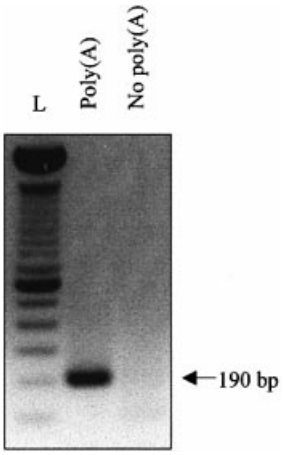

Fig. 4. The oligo(dT)$_{18}$-adapter primer cannot initiate cDNA synthesis at non-polyadenylated 3′ termini of atpA-orf522 transcripts. Negative image of an ethidium bromide-stained gel of PCR products amplified as in Figure 2 from cDNAs corresponding to non-polyadenylated or polyadenylated 3′ UTRs of atpA-orf522 mRNAs that have been *in vitro* transcribed using clone 3 in Figure 3 as DNA template. The presence or absence of a poly(A) tail in the RNA used for cDNA synthesis is indicated at the top of the lanes. The lane L corresponds to a 100 bp DNA ladder from Gibco-BRL.

sites within a short sequence of 12 nucleotides which spans the 3′ termini mapped in the RNase protection experiments (Figure 3). In view of the experiment presented in Figure 4, it seems very unlikely that non-specific priming of the oligo(dT)$_{18}$-adapter primer could have occurred only at the 3′ termini of the transcripts. The fourth reason is that in the regions 3′ to the *orf522* sequence where polyadenylation occurs, there are no A-rich sequences which could have allowed the artefactual priming of the oligo(dT)$_{18}$-adapter primer to unprocessed atpA-orf522 transcripts (Figure 3). The actual lengths of poly(A) tails are as yet undetermined (see Discussion), but the data presented in Figures 2 to 4 demonstrate that atpA-orf522 mRNAs may be polyadenylated *in vivo* at their 3′ termini.

atpA-orf522 transcripts are preferentially polyadenylated in male florets of the restored hybrid plants as compared with sterile plants

To check whether polyadenylation of mitochondrial mRNAs varies in different tissues, cDNA was synthesized from mitochondrial RNA isolated from cotyledons of 4-day-old, dark-grown seedlings and male florets from fertile, sterile and restored hybrid plants. In both these organs, PCR products corresponding to polyadenylated 3′ termini of atpA-orf522 transcripts were amplified (Figure 5). As an internal control to ensure that similar amounts of cDNAs were used for PCR amplification, PCR experiments were performed using an atp6-specific primer in combination with the adapter primer. These experiments revealed that, similar to atpA-orf522 transcripts, a polyadenylate sequence may be present at the predicted 3′ termini of atp6 transcripts. Equal amounts of atp6 PCR products were amplified using cDNAs prepared from cotyledon RNAs from sterile and restored hybrid seedlings (Figure 5D). Similarly, equal amounts of orf522 PCR products were amplified using cDNAs prepared from cotyledon RNAs from sterile and restored hybrid seedlings

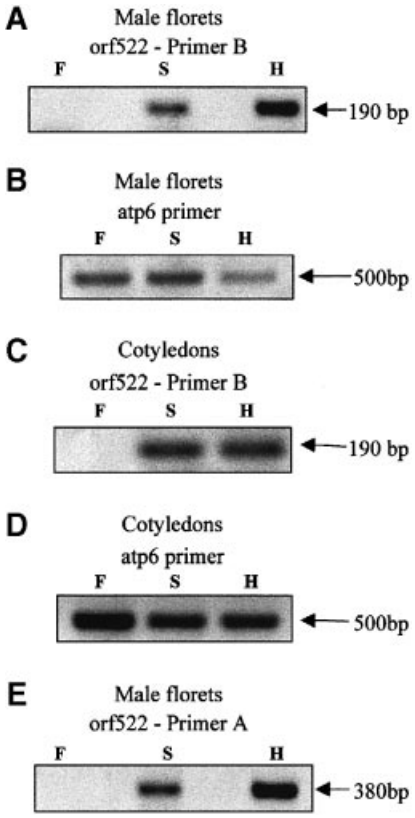

Fig. 5. Polyadenylation of atpA-orf522 transcripts is regulated during development in the restored hybrid plants. cDNAs were synthesized using the oligo(dT)$_{18}$-adapter primer from RNAs isolated from mitochondria of male florets or cotyledons from fertile (F), sterile (S) or restored hybrid (H) plants. The type of organ used for cDNA preparation and the primer used for the PCR experiments are indicated on the figure. Negative images of the relevant portions of ethidium bromide-stained gels are presented.

(Figure 5C). Interestingly, the amount of PCR product corresponding to polyadenylated atpA-orf522 transcripts is markedly increased for male florets from the restored hybrid plants as compared with sterile plants (Figure 5A). This difference is probably underestimated as the amount of atp6-specific PCR products is lower using cDNAs prepared from male florets of the restored hybrid plants as compared with sterile plants (Figure 5B). The increase in the amount of PCR products corresponding to the polyadenylated 3′ termini of atpA-orf522 transcripts in the restored hybrid male florets as compared with sterile florets was further confirmed by the use of another orf522-specific primer (primer A in Figure 3) (Figure 5E). This difference was observed in 10 independent PCR experiments using these two different orf522-specific primers (see Figures 2 and 5A, E for the results of three of these experiments).

To confirm this result, PCR master mixes containing the adapter primer and either the atp6-specific primer or the orf522-specific primer B were prepared and divided into four aliquots for each of the cDNAs prepared from male floret mitochondria of sterile and restored hybrid plants. A PCR corresponding to each cDNA was stopped after 20, 25, 30 and 35 cycles of amplification. PCR products were fractionated on agarose gels and stained with ethidium bromide. The fluorescence intensity of each signal was recorded using a Fluor-S MultiImager (Bio-

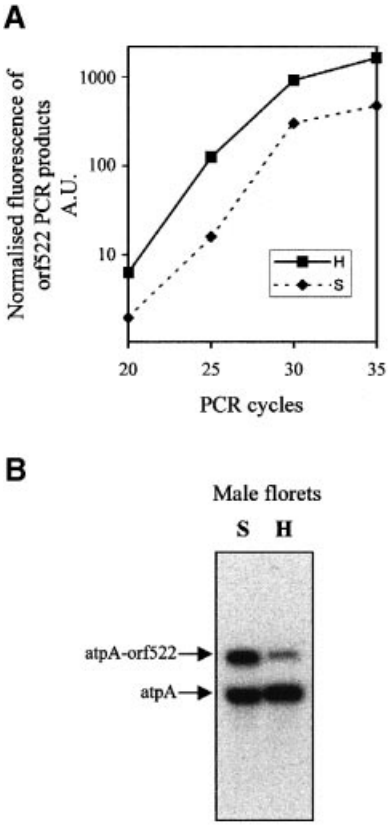

Fig. 6. The level of polyadenylated atpA-orf522 transcripts is higher in male florets of restored hybrid plants than of sterile plants. (**A**) Logarithmic representation of the fluorescence intensities of ethidium bromide-stained orf522 PCR products versus the number of PCR cycles. cDNAs were synthesized from RNAs isolated from male florets of sterile (S) or restored hybrid (H) plants and subjected to PCR amplification using the adapter primer in combination with the orf522-specific primer B or atp6-specific primer. The amounts of orf522 PCR products were normalized to the corresponding amounts of atp6 PCR products. (**B**) The steady-state level of atpA-orf522 transcripts is reduced in male florets of the restored hybrid plants. Total mitochondrial RNAs were extracted from mitochondria from male florets of sterile (S) and restored hybrid (H) plants and subjected to Northern blot analysis using an *atpA* probe.

Rad) and integrated using the Multi-Analyst software (Bio-Rad). Fluorescence intensities recorded for orf522 PCR products were normalized to the fluorescence intensities obtained for atp6 PCR products at a given number of PCR cycles and for a given cDNA sample. A logarithmic representation of the normalized fluorescence intensity for orf522 PCR products versus the number of PCR cycles is presented in Figure 6A. These integration data show that the amplification of both of the PCR products is exponential until 30 cycles and then reaches a plateau (Figure 6A). These data confirm that the level of polyadenylated atpA-orf522 transcripts is increased in male florets of the restored hybrid plants as compared with sterile plants (Figure 6A). This increase is tissue-specific as it is not observed in cotyledons (Figure 5C and D). The restored hybrid plants are obtained in a cross between the male sterile plants as female parents and 'restorer' plants (i.e. containing the restoration of fertility *Rf* genes) as male parents. Thus, as the sterile and the restored hybrid plants possess identical cytoplasm and equal proportion of the nuclear genomes of the sterile and restorer lines, we conclude that polyadenylation of atpA-orf522 transcripts is regulated in a tissue-specific manner by a nuclear gene(s). As the steady-state level of atpA-orf522 transcripts is markedly decreased in the male florets of restored hybrid plants as compared with sterile plants (Figure 6B), there is a positive correlation between the tissue-specific instability and increased polyadenylation of atpA-orf522 transcripts in the male florets of restored hybrid plants. This *in vivo* correlation suggests that polyadenylation could be involved in the degradation pathway of atpA-orf522 transcripts. To test this hypothesis, we then investigated the influence of the presence of poly(A) tails on RNA degradation by mitochondrial ribonucleases in an *in vitro* degradation system described below.

Polyadenylated RNA substrates can be degraded by two distinct RNase activities in sunflower mitochondria

None of the RNase activity(ies) involved in mRNA degradation in plant mitochondria has been identified to date. To study the possible effect of polyadenylation on the stability of atpA-orf522 mRNAs, we first characterized RNase activities in sunflower mitochondria. All the experiments presented here were performed three times using mitochondria isolated from etiolated cotyledons of restored hybrid seedlings and were then repeated using mitochondria isolated from male florets of restored hybrid plants as well as from potato tubers. We used a polyadenylated RNA substrate corresponding to the last 66 nucleotides of the 3′ UTR of atpA-orf522 transcripts followed by 19 adenosine residues (see Materials and methods). The polyadenylated RNA substrate was incubated with protein extracts corresponding to either the supernatant (matrix fraction) or the pellet (membrane fraction) of a low speed centrifugation (20 000 *g* for 15 min) of mitochondria that had been freeze–thawed five times. No RNase activity was detected in the matrix fraction under the conditions tested. However, the RNA substrate was rapidly degraded in the fraction corresponding to membrane proteins (see below). As several RNase activities could be present in this fraction, membrane proteins were solubilized with the detergent *n*-dodecyl-β-D-maltoside (DDM) and separated by FPLC on a MonoQ anion-exchange column (see Materials and methods). To assay for RNase activity, an aliquot of each FPLC fraction was incubated with the polyadenylated RNA substrate under the conditions described in the Materials and methods. The results obtained for the column fractions containing RNase activity are presented in Figure 7A. Interestingly, two distinct patterns of discrete degradation intermediates are clearly distinguishable in the different fractions (see for instance fraction F14 versus fraction F22 in Figure 7A). This indicates that either two distinct RNase activities are separated on the column or that the salt concentration influences the pattern of degradation of the RNA substrate by a single RNase activity. This latter possibility was eliminated in a subsequent experiment in which the salt concentration of the fractions F15 and F22 was adjusted to 480 mM for both samples (results not shown). The RNase activity 1 is eluted in fractions F13–F19 (salt concentration from 50 to 250 mM), whereas the RNase activity 2 is eluted in fractions F17–F27 (salt concentration from 160 to 500 mM) (Figure 7A). To avoid cross-

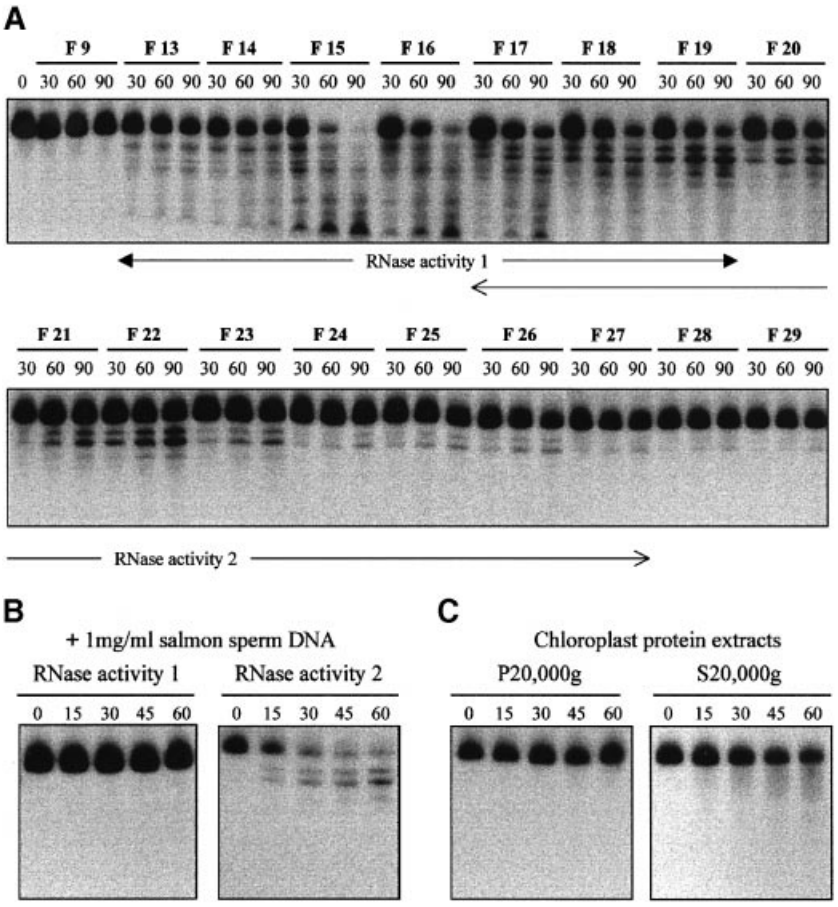

Fig. 7. Polyadenylated RNA substrate can be degraded by two distinct RNase activities. (**A**) Patterns of degradation intermediates obtained by incubating a polyadenylated RNA substrate with aliquots of membrane protein fractions separated on a MonoQ column as described in Materials and methods. The incubation time is indicated in minutes at the top of each lane. (**B**) Effect of competitor DNA on both RNase activities. Except for the presence of 1 mg/ml salmon sperm DNA, the experiment was conducted as in (A). (**C**) RNase activities 1 and 2 are not due to a contamination from chloroplasts. Purified chloroplasts (500 μg proteins) were treated as indicated for the mitochondrial samples in the Materials and methods and incubated with the polyadenylated RNA substrate. At the time indicated in minutes at the top of each lane, RNA from aliquots of the reaction was extracted with phenol-chloroform, precipitated by ethanol and run on denaturing acrylamide gels as in (A) and (B).

contamination between these two RNase activities in the following experiments, the fraction F15 was chosen as a source of RNase activity 1 and pooled fractions F22–F24 as a source of RNase activity 2. The RNase activity 1 was consistently more active than the RNase activity 2 in different experiments. Thus, to obtain a similar degradation rate of the polyadenylated substrate by the two RNase activities, Fractions 22–24 were concentrated 5-fold by ultrafiltration. In addition to their distinct patterns of degradation intermediates, the RNase activities could also be distinguished when the polyadenylated RNA substrate was incubated in the presence of DNA. As shown in Figure 7B, the RNase activity 1 is completely inhibited by the presence of DNA whereas the RNase activity 2 is not affected. Identical results were obtained when using the two RNase activities purified from potato mitochondria. These results show that at least two distinct RNase activities are present in both sunflower and potato mitochondria.

To rule out the possibility of contaminating plastid ribonucleases, the following experiment was performed. Chloroplasts were purified from young sunflower leaves and treated as were the samples of purified mitochondria (see Materials and methods). As shown in Figure 7C, the polyadenylated RNA substrate was not degraded in the chloroplast protein extract corresponding to the pellet of the 20 000 *g* centrifugation. The RNA substrate was degraded in the soluble chloroplast protein extract. However, none of the characteristic intermediates of degradation generated by either of the two mitochondrial RNase activities were observed. This experiment shows that neither of the two RNase activities described above is a contaminant from chloroplasts.

The RNase activity 2 preferentially degrades polyadenylated RNA substrates as compared with non-polyadenylated RNA substrates

To test whether polyadenylation influences the degradation rate of the RNA substrate by the mitochondrial ribonucleases, each RNase activity was separately incubated with a non-polyadenylated RNA substrate, a polyadenylated RNA substrate or both substrates together. The non-polyadenylated RNA substrate is identical to the previously described polyadenylated one except that it lacked any adenosine residues at its 3′ terminus (see Materials and methods). As shown in Figure 8A, the RNase activity 1 degrades both polyadenylated and non-polyadenylated substrates at the same rate. Strikingly, the non-polyadenyl-

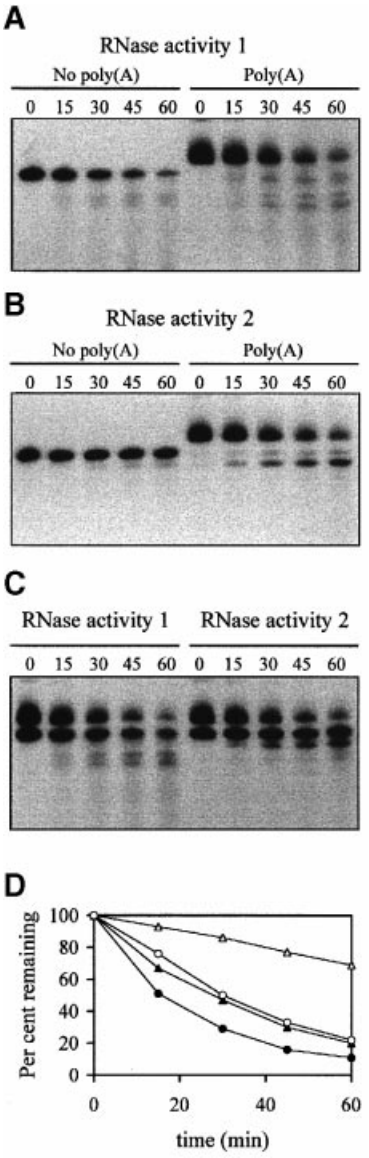

Fig. 8. Influence of polyadenylation on the degradation of RNA substrates by the two RNase activities. Non-polyadenylated and/or polyadenylated RNA substrates were incubated separately with the RNase activities 1 and 2 as indicated on the top of each panel. The incubation time is indicated in minutes at the top of each lane. (**A**) RNase activity 1. (**B**) RNase activity 2. (**C**) RNase activities 1 and 2 were incubated separately with both non-polyadenylated and polyadenylated substrates. (**D**) Radioactive counts corresponding to full-length RNA substrates were recorded in three experiments and plotted against time. Non-polyadenylated (triangles) and polyadenylated (circles) RNA substrates were incubated with RNase activity 1 (filled symbols) or RNase activity 2 (open symbols).

ated substrate was relatively stable when incubated with the RNase activity 2 whereas the polyadenylated RNA substrate was degraded (Figure 8B). The same result was obtained when both types of substrates were incubated together with each RNase activity (Figure 8C and D). The radioactive counts corresponding to full-length RNA substrates were determined in three experiments using a GS-525 Molecular Imager System (Bio-Rad). These data show that the RNase activity 2 degrades the polyadenylated RNA substrate three times faster than the non-polyadenylated one (Figure 8D). Similar results were obtained using polyadenylated and non-polyadenylated RNA substrates corresponding to the 3′ terminal 14 nucleotides of the orf522 open reading frame and 128 nucleotides of the 3′ UTR of atpA-orf522 transcripts (clone 3 in Figure 3) (results not shown).

Discussion

The molecular mechanisms involved in the degradation of plant mitochondrial mRNAs are still largely unknown. A recent report has demonstrated that the presence or absence of a secondary structure(s) located at the 3′ end of a mitochondrial transcript determine its stability (Bellaoui *et al*., 1997). In addition to this mechanism for controlling mRNA stability in mitochondria, we show here by exploiting the CMS system in sunflower that a plant mitochondrial mRNA may be polyadenylated at its 3′ end and that polyadenylation enhances the degradation rate of RNA substrates by an RNase activity that is membrane-bound. In addition, we show that polyadenylation of atpA-orf522 transcripts is developmentally regulated by a nuclear gene(s) upon restoration of fertility.

Length of poly(A) tracts in plant mitochondrial mRNAs

The length of poly(A) tails varies between 14 and 60 nucleotides in bacterial RNAs (Ohara *et al*., 1995; Ingle and Kushner, 1996; Cao and Sarkar, 1997) and can be as long as several hundred nucleotides in the mRNAs of chloroplasts (Lisitsky *et al*., 1996). In the latter case, the poly(A) moiety is mostly composed of adenosines (70%), but also contains guanosines (25%) and more rarely cytidines and uridines (5%) (Lisitsky *et al*., 1996). In order to investigate the presence of poly(A) tails in plant mitochondrial mRNAs in this study, we have employed a RT–PCR strategy previously used by others to determine the position of polyadenylation sites in chloroplast (Kudla *et al*., 1996) and yeast cytoplasmic RNAs (Sparks and Dieckmann, 1998). These authors used oligo(dT) primers of 18 or 17 nucleotides, respectively, to prime cDNA synthesis and the cloned poly(A) tails recovered were between 18 and 35 nucleotides (Kudla *et al*., 1996) and 15 and 30 nucleotides (K.A.Sparks and C.L.Dieckmann, personal communication), respectively, as compared with the longer poly(A) tails present *in vivo*. Thus this method is efficient in determining the presence of poly(A) tails but does not allow a precise determination of their lengths *in vivo*. In this study, our results demonstrate the existence of poly(A) tails in sunflower mitochondrial atpA-orf522 mRNAs (Figures 2–5) but their exact length *in vivo* remains to be determined, as does the proportion of a given mRNA species which is polyadenylated. However, our data show that poly(A) sequences of 19 nucleotides are sufficient to accelerate the degradation of RNA substrates by one of the two RNase activities that we have characterized (Figure 8).

Nuclear restoration of fertility in CMS sunflower and control of atpA-orf522 mRNA polyadenylation

It has previously been shown that atpA-orf522 transcripts associated with CMS in sunflower are preferentially destabilized in a tissue-specific manner upon the introduction of a nuclear restorer gene(s) (Monéger *et al*., 1994). Here, we show that this preferential degradation is associated

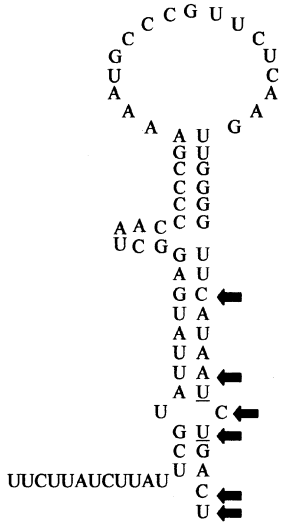

Fig. 9. Predicted secondary structure at the 3′ end of atpA-orf522 transcripts and position of polyadenylation sites. The secondary structure prediction was performed using the MFOLD program of the GCG Wisconsin package, version 8.1.0. The nucleotides corresponding to the mapped 3′ extremities of atpA-orf522 transcripts are underlined and the position of the polyadenylation sites are indicated by arrows.

with an increased proportion of the atpA-orf522 transcripts that are polyadenylated in restored hybrid versus sterile florets. Furthermore, polyadenylation induces the degradation of polyadenylated RNA substrates by the RNase activity 2 which is present in sunflower mitochondria. The specific control of polyadenylation of atpA-orf522 mRNAs in male florets of the restored hybrid plants is thus possibly linked to the action of at least one of the gene products of the two restorer loci, shown to be present in restored hybrid plants. Polyadenylation of atpA-orf522 transcripts could either be the primary cause of the control of instability or a consequence of the targeting of these transcripts for degradation.

Elements controlling the stability of atpA-orf522 transcripts

A secondary structure predicted to fold into a stem–loop is present at the 3′ end of atpA-orf522 mRNAs (Figure 9). Interestingly, the majority of polyadenylation sites are located at the base of the double-stranded structure (Figure 9). As secondary structures at the 3′ termini have been shown to be important determinants of plant mitochondrial mRNA stability (Bellaoui *et al*., 1997), it is possible that polyadenylation facilitates the degradation of such structures by providing a 'toehold' for the RNase activity 2. Indeed, in bacteria, such a role for poly(A) tails has been demonstrated in the absence of RNase E for one bacterial exonuclease, PNPase (Coburn and Mackie, 1996). Most, but not all, bacterial and chloroplast mature transcripts terminate with a stem–loop structure. Both in bacteria and chloroplasts, these structures are poor substrates for polyadenylation. The major, but not unique, mechanism by which bacterial RNAs are degraded seems to involve endonucleolytic cleavages by RNase E which generate 3′ extremities that are then polyadenylated and degraded by 3′ to 5′ exonucleases such as PNPase and RNase II. A protein complex termed the degradosome, which is involved in bacterial RNA degradation, is composed of RNase E, PNPase, RhlB (an RNA helicase), enolase (a glycolytic enzyme which has an unknown role in the degradosome) and DnaK (Carpousis *et al*., 1994; Miczak *et al*., 1996; Py *et al*., 1996). It has also been reported that GroEL could be part of this complex (Sohlberg *et al*., 1993; Miczak *et al*., 1996). A closely related protein complex characterized in chloroplasts contains homologues of PNPase (100RNP) and RNase E (p67) (Hayes *et al*., 1996). Indeed, the degradation of the chloroplast mRNAs that has been investigated so far (i.e. *petD*, *psbA* and *psaA-psaB-rps14* mRNAs) is initiated by endonucleolytic cleavages (Klaff, 1995; Kudla *et al.*, 1996; Lisitsky *et al.*, 1996). The 100RNP/PNPase binds to and preferentially degrades poly(A) RNAs (Lisitsky *et al*., 1997a). Interestingly, 100RNP/PNPase has also been found associated with a poly(A) polymerase activity in chloroplasts (Li *et al*., 1998). We have so far failed to identify polyadenylated RNAs generated from endonucleolytic cleavage within the 3′ 217 nucleotides of the orf522 open reading frame and the 3′ UTR of the atpA-orf522 transcripts. It thus seems that polyadenylation of atpA-orf522 transcripts is not triggered by the removal of the stem–loop structure or of a sequence necessary for the interaction with stabilizing proteins at the 3′ end of these transcripts.

At least two distinct RNase activities are associated with sunflower and potato mitochondrial membranes

Our results show that at least two distinct RNase activities that can degrade polyadenylated RNA substrates are associated with sunflower and potato mitochondrial membranes. The RNase activity 1 is recovered in the fraction corresponding to membrane proteins, is the most active ribonuclease in mitochondria at least under the conditions tested (Figure 7A), is inhibited by DNA (Figure 7B) and is ATP-independent (results not shown). All these characteristics are shared with a non-specific nuclease activity that is present in yeast mitochondria. This nuclease activity in yeast is due to the *NUC1* gene product, which is responsible for >50% of the total cellular nuclease activity in *Saccharomyces cerevisae* and exhibits both DNase and RNase activities (Dake *et al*., 1988). Nuc1p is associated with the inner mitochondrial membrane and its role is still not precisely understood since a null allele of the *NUC1* gene does not result in any obvious phenotype (Dake *et al*., 1988; Zassenhaus *et al*., 1988). However, it has recently been demonstrated that Nuc1p is not involved in the processing and turnover of mitochondrial transcripts (Dziembowski *et al.*, 1998). It may be inferred that this enzyme activity must be tightly controlled *in vivo*. We do not yet know whether the plant mitochondrial RNase activity 1 is related to the yeast Nuc1p and/or if it plays any role in the degradation of plant mitochondrial mRNAs (see below). In contrast to the RNase activity 1, the RNase activity 2 preferentially degrades polyadenylated versus non-polyadenylated RNA substrates *in vitro* (Figure 8). Therefore, we propose that this activity is likely to be involved in the control of degradation of plant mitochondrial mRNAs. The intermediates of degradation are clearly different between the RNase activities 1 and 2 (Figures 7 and 8), indicating that these enzymes could play a complementary role in the complete degradation of an

RNA substrate. The RNase activity 2 could initiate the degradation of a transcript after polyadenylation of the 3′ ends, after which the RNase activity 1 could be involved in the further degradation of the intermediates generated by the RNase activity 2. This RNase activity 2 is present in sunflower as well as in potato mitochondria and identical properties and patterns of degradation intermediates were observed between the two plant species using RNA substrates corresponding to the 3′ UTR of atpA-orf522 transcripts. Thus, the polyadenylation-mediated degradation of RNA substrates by the RNase activity 2 is not a phenomenon restricted to sunflower mitochondria but rather reflects a more general process in plant mitochondria.

The next steps in understanding the molecular mechanisms of plant mitochondrial mRNA degradation will involve the identification of the proteins responsible for polyadenylation and degradation of mitochondrial transcripts. The *in vitro* RNA degradation system described in this paper (Figures 7 and 8) represents an assay system to allow the purification of the RNase activity responsible for the degradation of polyadenylated transcripts in plant mitochondria. A complementary approach to identifying these proteins is to look for plant homologues of proteins already identified in systems much better characterized at the genetic level, such as bacteria, chloroplasts and yeast mitochondria. Interestingly, we have shown that a plant homologue of the yeast Suv3 protein is imported into plant mitochondria (D.Gagliardi, U.Spadinger, J.Kuhn, A.Brennicke, C.J.Leaver and S.Binder, manuscript in preparation). Suv3p is an RNA helicase that is part of a protein complex, mtEXO, responsible for RNA degradation in yeast mitochondria (Min and Zassenhaus, 1993; Margossian *et al*., 1996). The product of the yeast *DSS-1* gene shares some homologies with the bacterial RNase II and is probably part of the mtEXO complex (Dmochowska *et al*., 1995; Dziembowski *et al*., 1998). The existence of a plant mitochondrial Suv3p homologue raises the possibility that a related complex exhibiting ribonuclease activity could be present in plant mitochondria.

Materials and methods

Plant material

Sunflower lines and plant growth conditions are described in Smart *et al*. (1994). Sunflower mitochondria were isolated from 4-day-old etiolated seedlings and from 1 to 1.5 mm male florets which correspond to premeiotic to pachytene meiotic stages (Smart *et al*., 1994). Mitochondria were isolated by differential centrifugation and purification on Percoll gradients.

Northern blot analysis and RNase protection experiments

Mitochondrial RNA and total cellular RNA from etiolated seedlings or male florets were isolated using the Trizol reagent (Gibco-BRL). Northern blot experiments were performed as described in Monéger *et al*. (1994). For RNase protection experiments, a cloned *Bam*HI–*Hin*cII mitochondrial DNA fragment containing the last 214 nucleotides of the *orf522* open reading frame plus the region 3′ of the *orf522* gene was digested by *Bbv*I (probe A), *Sca*I (probe B) or *Bam*HI (probe C) restriction enzymes prior to synthesizing *in vitro* antisense RNA using the T3 RNA polymerase (Promega). The *in vitro* transcribed RNA (2×10^5 c.p.m.) were hybridized to 50 μg of total RNA from male florets of fertile, sterile and restored hybrid plants. Only the relevant portion of the autoradiograph obtained using the antisense probe A is shown. No other bands were detected on the autoradiograph of the total gel. To determine the sizes of the protected RNA fragments, unrelated *in vitro* transcribed RNAs of known lengths were run alongside a DNA sequencing reaction to normalize the length of RNA to a ladder of DNA fragments.

cDNA synthesis and PCR amplification

Total mitochondrial RNAs (50 μg) from cotyledons or male florets were incubated with 10 U of DNase I for 30 min at 37°C. After phenol/chloroform extraction and ethanol precipitation, RNAs were reverse-transcribed using an oligo$(dT)_{18}$-adapter primer (Table I) and Mu-MLV reverse transcriptase (Stratagene). Aliquots of cDNA reactions were subjected to PCR amplification using the adapter primer in combination with a gene-specific primer (Table I) and Red-Taq DNA polymerase (Sigma). Unless otherwise indicated, PCR amplification was performed using 30 cycles of 1 min at 94, 50 and 72°C followed by one step of 5 min at 72°C. PCR products were fractionated on 1.5% (w/v) agarose gels and stained with ethidium bromide. Fluorescence was recorded using a Fluor-S MultiImager (Bio-Rad) and integrated using the Multi-Analyst software (Bio-Rad). PCR products amplified using the adapter primer and the orf522-specific primer B were cloned in the *Kpn*I and *Bam*HI sites of pBluescript KS^+ plasmid. Sequence data were obtained using an ABI 310 sequencer (Perkin-Elmer). Unfortunately, we could not determine whether the monocistronic atpA transcripts are polyadenylated as there is a A-rich region immediately 3′ to the stop codon which is primed by the oligo$(dT)_{18}$-adapter primer (results not shown).

Separation of the two RNase activities by FPLC

Frozen mitochondrial pellets were resuspended at a concentration of 5 mg protein/ml in 25 mM KH_2PO_4 pH 6.7, 2 mM dithiothreitol (DTT) and freeze–thawed five times. The mitochondrial lysate was centrifuged at 20 000 *g* for 15 min at 4°C. The membrane protein pellet was resuspended at a concentration of 20 mg/ml in 25 mM MOPS, pH 7.5. The detergent DDM was added to a final concentration of 1% (w/v) and the suspension was gently rotated for 1 h at 4°C. Insoluble material was removed by centrifugation at 20 000 *g* for 15 min at 4°C. The supernatant was adjusted to 0.1% DDM and injected onto a 1 ml MonoQ column (Pharmacia) previously equilibrated in 25 mM MOPS pH 7.5, 0.1% DDM (w/v) (buffer A). We used from 5 to 20 mg of membrane proteins per run. The column was washed with 17 ml of buffer A and a linear gradient from 0 to 650 mM NaCl in buffer A was developed over a period of 18 min at a flow rate of 1 ml/min. The first 11 fractions were collected as 1.5 ml fractions and the subsequent ones as 1 ml fractions. Aliquots of fractions were frozen in liquid nitrogen and stored at –80°C. Up to five cycles of freezing and thawing did not affect either of the RNase activities.

In vitro RNA degradation assays

Clone 5 in Figure 3 was used as PCR template using the reverse primer of the pBluescript plasmid and the orf522-specific primer C (Table I). PCR products were cloned into the *Kpn*I and *Bam*HI sites of the pBluescript KS^+ plasmid. This plasmid was then used as template to produce both polyadenylated and non-polyadenylated substrates. The non-polyadenylated RNA substrate was generated from PCR products amplified using the M13 –20 primer of pBluescript KS^+ and the orf522-specific primer D (Table I). The PCR products were digested with the *Xho*I restriction enzyme. The polyadenylated substrate was generated from PCR products amplified using the M13 –20 primer of pBluescript KS^+ and the adapter primer (Table I). PCR products were digested using the *Alw*I restriction enzyme. Both RNA substrates were synthesized using the T3 RNA polymerase (Promega) and labelled using [α^{32}P]UTP.

In the experiment presented in Figure 7A, 10 mg of membrane proteins from sunflower cotyledon mitochondria were injected on a MonoQ column. Ten microlitre aliquots of FPLC fractions were supplemented with 1 mM ATP and 0.4 mM DTT and incubated with the radiolabelled RNA substrates. At the indicated time, 3 μl aliquots of the degradation reactions were removed, added to 5 μl of formamide and fractionated on 8% (w/v) acrylamide/7 M urea gels. The dried gels were exposed to X-ray film. For the subsequent experiments, the RNase activity 2 contained in fractions F22–F24 was concentrated five times by ultrafiltration by using Vivaspin 500 μl concentrators (Vivascience) with a membrane cut-off of 10 kDa.

Acknowledgements

We would like to thank Janneke Balk for the chloroplast samples and Dr A.H.Millar for potato mitochondrial membrane samples and for discussion on protein chromatography. This work was supported by the Biotechnology and Biological Sciences Research Council (reference G05136).

References

Bellaoui,M., Pelletier,G. and Budar,F. (1997) The steady-state level of mRNA from the Ogura cytoplasmic male sterility locus in *Brassica* cybrids is determined post-transcriptionally by its 3′ region. *EMBO J.*, **16**, 5057–5068.

Bhat,G.J., Souza,A.E., Feagin,J.E. and Stuart,K. (1992) Transcript-specific developmental regulation of polyadenylation in *Trypanosoma brucei* mitochondria. *Mol. Biochem. Parasitol.*, **52**, 231–240.

Cao,G.J. and Sarkar,N. (1997) Stationary phase-specific mRNAs in *Escherichia coli* are polyadenylated. *Biochem. Biophys. Res. Commun.*, **239**, 46–50.

Carpousis,A.J., Vanhouwe,G., Ehretsmann,C. and Krisch,H.M. (1994) Copurification of *Escherichia coli* RNAse-E and PNPase—Evidence for a specific association between 2 enzymes important in RNA processing and degradation. *Cell*, **76**, 889–900.

Coburn,G.A. and Mackie,G.A. (1996) Differential sensitivities of portions of the mRNA for ribosomal protein S20 to 3′-exonucleases dependent on oligoadenylation and RNA secondary structure. *J. Biol. Chem.*, **271**, 15776–15781.

Dake,E., Hofmann,T.J., McIntire,S., Hudson,A. and Zassenhaus,H.P. (1988) Purification and properties of the major nuclease from mitochondria of *Saccharomyces cerevisiae*. *J. Biol. Chem.*, **263**, 7691–7702.

Dmochowska,A., Golik,P. and Stepien,P.P. (1995) The novel nuclear gene *Dss-1* of *Saccharomyces cerevisiae* is necessary for mitochondrial biogenesis. *Curr. Genet.*, **28**, 108–112.

Dombrowski,S., Brennicke,A. and Binder,S. (1997) 3′-inverted repeats in plant mitochondrial mRNAs are processing signals rather than transcription terminators. *EMBO J.*, **16**, 5069–5076.

Dziembowski,A., Malewicz,M., Minczuk,M., Golik,P., Dmochowska,A. and Stepien,P.P. (1998) The yeast nuclear gene *DSS1*, which codes for a putative RNase II, is necessary for the function of the mitochondrial degradosome in processing and turnover of RNA. *Mol. Gen. Genet.*, **260**, 108–114.

Finnegan,P.M. and Brown,G.G. (1990) Transcriptional and post-transcriptional regulation of RNA levels in maize mitochondria. *Plant Cell*, **2**, 71–83.

Haugel-Nielsen,J., Hajnsdorf,E. and Regnier,P. (1996) The rpsO mRNA of *Escherichia coli* is polyadenylated at multiple sites resulting from endonucleolytic processing and exonucleolytic degradation. *EMBO J.*, **15**, 3144–3152.

Hayes,R., Kudla,J., Schuster,G., Gabay,L., Maliga,P. and Gruissem,W. (1996) Chloroplast mRNA 3′-end processing by a high molecular weight protein complex is regulated by nuclear encoded RNA binding proteins. *EMBO J.*, **15**, 1132–1141.

Hendler,F.J., Padmanaban,G., Patzer,J., Ryan,R. and Rabinowitz,M. (1975) Yeast mitochondrial RNA contains a short polyadenylic acid segment. *Nature*, **258**, 357–359.

Ingle,C.A. and Kushner,S.R. (1996) Development of an *in vitro* mRNA decay system for *Escherichia coli*: Poly(A) polymerase I is necessary to trigger degradation. *Proc. Natl Acad. Sci. USA*, **93**, 12926–12931.

Janska,H., Sarria,R., Woloszynska,M., ArrietaMontiel,M. and Mackenzie,S.A. (1998) Stoichiometric shifts in the common bean mitochondrial genome leading to male sterility and spontaneous reversion to fertility. *Plant Cell*, **10**, 1163–1180.

Klaff,P. (1995) mRNA decay in spinach chloroplasts: psbA mRNA degradation is initiated by endonucleolytic cleavages within the coding region. *Nucleic Acids Res.*, **23**, 4885–4892.

Köhler,R.H., Horn,R., Lossl,A. and Zetsche,K. (1991) Cytoplasmic male-sterility in sunflower is correlated with the cotranscription of a new open reading frame with the *atpA* gene. *Mol. Gen. Genet.*, **227**, 369–376.

Koslowsky,D.J. and Yahampath,G. (1997) Mitochondrial mRNA 3′ cleavage polyadenylation and RNA editing in *Trypanosoma brucei* are independent events. *Mol. Biochem. Parasitol.*, **90**, 81–94.

Kudla,J., Hayes,R. and Gruissem,W. (1996) Polyadenylation accelerates degradation of chloroplast mRNA. *EMBO J.*, **15**, 7137–7146.

Laver,H.K., Reynolds,S.J., Monéger,F. and Leaver,C.J. (1991) Mitochondrial genome organization and expression associated with cytoplasmic male-sterility in sunflower (*Helianthus annuus*). *Plant J.*, **1**, 185–193.

Li,Q.S., DasGupta,J. and Hunt,A.G. (1998) Polynucleotide phosphorylase is a component of a novel plant poly(A) polymerase. *J. Biol. Chem.*, **273**, 17539–17543.

Lisitsky,I., Klaff,P. and Schuster,G. (1996) Addition of destabilizing poly(A)-rich sequences to endonuclease cleavage sites during the degradation of chloroplast mRNA. *Proc. Natl Acad. Sci. USA*, **93**, 13398–13403.

Lisitsky,I., Kotler,A. and Schuster,G. (1997a) The mechanism of preferential degradation of polyadenylated RNA in the chloroplast—The exoribonuclease 100RNP/polynucleotide phosphorylase displays high binding affinity for poly(A) sequence. *J. Biol. Chem.*, **272**, 17648–17653.

Lisitsky,I., Klaff,P. and Schuster,G. (1997b) Blocking polyadenylation of mRNA in the chloroplast inhibits its degradation. *Plant J.*, **12**, 1173–1178.

Manley,J.L. and Proudfoot,N.J. (1994) RNA 3′ ends—Formation and function. *Genes Dev.*, **8**, 259–264.

Margossian,S.P., Li,H.L., Zassenhaus,H.P. and Butow,R.A. (1996) The DExH box protein Suv3p is a component of a yeast mitochondrial 3′-to-5′ exoribonuclease that suppresses group I intron toxicity. *Cell*, **84**, 199–209.

Miczak,A., Kaberdin,V.R., Wei,C.L. and LinChao,S. (1996) Proteins associated with RNase E in a multicomponent ribonucleolytic complex. *Proc. Natl Acad. Sci. USA*, **93**, 3865–3869.

Min,J.J. and Zassenhaus,H.P. (1993) A nucleoside triphosphate-regulated, 3′ exonucleolytic mechanism is involved in turnover of yeast mitochondrial RNAs. *J. Bacteriol.*, **175**, 6245–6253.

Monéger,F., Smart,C.J. and Leaver,C.J. (1994) Nuclear restoration of cytoplasmic male-sterility in sunflower is associated with the tissue-specific regulation of a novel mitochondrial gene. *EMBO J.*, **13**, 8–17.

Mulligan,R.M., Leon,P. and Walbot,V. (1991) Transcriptional and posttranscriptional regulation of maize mitochondrial gene-expression. *Mol. Cell. Biol.*, **11**, 533–543.

Ohara,E.B., Chekanova,J.A., Ingle,C.A., Kushner,Z.R., Peters,E. and Kushner,S.R. (1995) Polyadenylation helps regulate messenger-RNA decay in *Escherichia coli*. *Proc. Natl Acad. Sci. USA*, **92**, 1807–1811.

Ojala,D., Montoya,J. and Attardi,G. (1981) tRNA punctuation model of RNA processing in human mitochondria. *Nature*, **290**, 470–474.

Py,B., Higgins,C.F., Krisch,H.M. and Carpousis,A.J. (1996) A DEAD-box RNA helicase in the *Escherichia coli* RNA degradosome. *Nature*, **381**, 169–172.

Sarkar,N. (1997) Polyadenylation of mRNA in prokaryotes. *Annu. Rev. Biochem.*, **66**, 173–197.

Schnable,P.S. and Wise,R.P. (1998) The molecular basis of cytoplasmic male sterility and fertility restoration. *Trends Plant Sci.*, **3**, 175–180.

Schuster,W., Hiesel,R., Isaac,P.G., Leaver,C.J. and Brennicke,A. (1986) Transcript termini of messenger-RNAs in higher-plant mitochondria. *Nucleic Acids Res.*, **14**, 5943–5954.

Smart,C.J., Monéger,F. and Leaver,C.J. (1994) Cell-specific regulation of gene-expression in mitochondria during anther development in sunflower. *Plant Cell*, **6**, 811–825.

Söderbom,F. and Wagner,E.G.H. (1998) Degradation pathway of CopA, the antisense RNA that controls replication of plasmid R1. *Microbiology*, **144**, 1907–1917.

Sohlberg,B., Lundberg,U., Hartl,F.U. and VonGabain,A. (1993) Functional interaction of heat-shock protein GroEL with an RNase E-like activity in *Escherichia coli*. *Proc. Natl Acad. Sci. USA*, **90**, 277–281.

Sparks,K.A. and Dieckmann,C.L. (1998) Regulation of poly(A) site choice of several yeast mRNAs. *Nucleic Acids Res.*, **26**, 4676–4687.

Szalewska-Palasz,A., Wrobel,B. and Wegrzyn,G. (1998) Rapid degradation of polyadenylated oop RNA. *FEBS Lett.*, **432**, 70–72.

Xu,F.F. and Cohen,S.N. (1995) RNA degradation in *Escherichia coli* regulated by 3′ adenylation and 5′ phosphorylation. *Nature*, **374**, 180–183.

Zassenhaus,H.P., Hofmann,T.J., Uthayashanker,R., Vincent,R.D. and Zona,M. (1988) Construction of a yeast mutant lacking the mitochondrial nuclease. *Nucleic Acids Res.*, **16**, 3283–3296.

Received April 1, 1999; revised and accepted May 18, 1999

Note added in proof

Polyadenylation of the mitochondrial COX2 mRNA has been characterized in maize (D.S.Lupold, A.G.F.S.Caoile and D.B.Stein, in preparation).